UNITED STATES
DEPARTMENT OF THE INTERIOR
GEOLOGICAL SURVEY
WASHINGTON, D.C. 20242

Interagency Report
NASA-113
September 1968

DRF-06206

Mr. Robert Porter
Acting Program Chief,
Earth Resources Survey
Code SAR - NASA Headquarters
Washington, D.C. 20546

Dear Bob:

Transmitted herewith is one copy of:

INTERAGENCY REPORT NASA-113

GEOLOGIC EVALUATION OF THERMAL INFRARED IMAGERY,

CALIENTE AND TEMBLOR RANGES, SOUTHERN CALIFORNIA*

by

Edward W. Wolfe**

Sincerely yours,

William A. Fischer
Research Coordinator
EROS Program

*Work performed under NASA Contract No. W-12589 and Task No. 160-75-(

**U.S. Geological Survey, Flagstaff, Arizona

UNITED STATES

DEPARTMENT OF THE INTERIOR

GEOLOGICAL SURVEY

INTERAGENCY REPORT NASA-113

GEOLOGIC EVALUATION OF THERMAL INFRARED IMAGERY, CALIENTE AND TEMBLOR RANGES, SOUTHERN CALIFORNIA*

by

Edward W. Wolfe**

September 1968

Prepared by the Geological Survey
for the National Aeronautics and
Space Administration (NASA)

*Work performed under NASA Contract No. W-12589 and Task No. 160-75-01-44-10
**U.S. Geological Survey, Flagstaff, Arizona

FOREWORD

The infrared imagery (8-13 micron) and photography described in this report were acquired by the NASA Convair 240 on Mission 8 in June 1965. Ground data acquisition, conducted during May and October 1967, was aimed at determining the reasons for anomalous conditions revealed on the imagery; this study was part of the Geologic Applications Program Task entitled Ground Truth Investigations - NASA No. 160-75-01-44-10.

CONTENTS

ILLUSTRATIONS

ILLUSTRATIONS (CONTINUED)

Geologic Evaluation of Thermal Infrared Imagery, Caliente and Temblor Ranges, Southern California

by

Edward W. Wolfe

U.S. Geological Survey

345 Middlefield Road, Menlo Park, Calif.

ABSTRACT

Thermal infrared (8 to 13 micron) imagery was obtained in the Caliente and Temblor Ranges and Carrizo Plain, southern California, in the pre-dawn and post-sunrise hours of June 18, 1965. Field observations; measurements of moisture and specific gravity of the regolith, and radiation temperatures; and comparison with geologic maps and aerial photographs lead to the following conclusions:

(1) The specific gravities of surficial materials (usually not bedrock) influence tonal densities in the pre-dawn imagery.

(2) Geologic interpretation of tonal density patterns is complicated by topographic, atmospheric, and vegetative effects on pre-dawn radiation.

(3) Geologic features such as outcrop patterns and some faults are recognizable in the infrared imagery as well as in aerial photographs. The sensitivity of the system to microclimatic anomalies may be valuable in aiding recognition of some geologic features with subtle topographic expression.

(4) Local radiative anomalies, previously suggested to be caused by the occurrence of ground water at shallow depths, may be caused by night-time entrapment of cold air in poorly drained, topographically low areas.

(5) Post-sunrise imagery is dominated by the preferential warming of slopes exposed to the early morning sun and resembles low sun angle photographs.

Introduction

Thermal infrared imagery, recording radiation from 8 to 13 microns in wavelength, was flown by NASA on June 18, 1965 in the Carrizo Plain of southern California. A line approximately normal to the regional geologic structure was selected for detailed analysis and is shown in figure 1. Localities at which supplemental observations were made are

---

Figure 1 near here

---

also shown in figure 1. A preliminary report on imagery from the Carrizo Plain was made by Wallace and Moxham (1966, 1967). A published geologic map by Vedder and Repenning (1965) was extensively used in the Caliente Range, and unpublished maps by both T. W. Dibblee and J. G. Vedder were used to evaluate the imagery in the Temblor Range.

Figure 2 is a generalized geologic map of the area in which imagery

---

Figure 2 near here

---

was studied in detail. The stratigraphic nomenclature used on the map and in this report is that of Dibblee (1962).

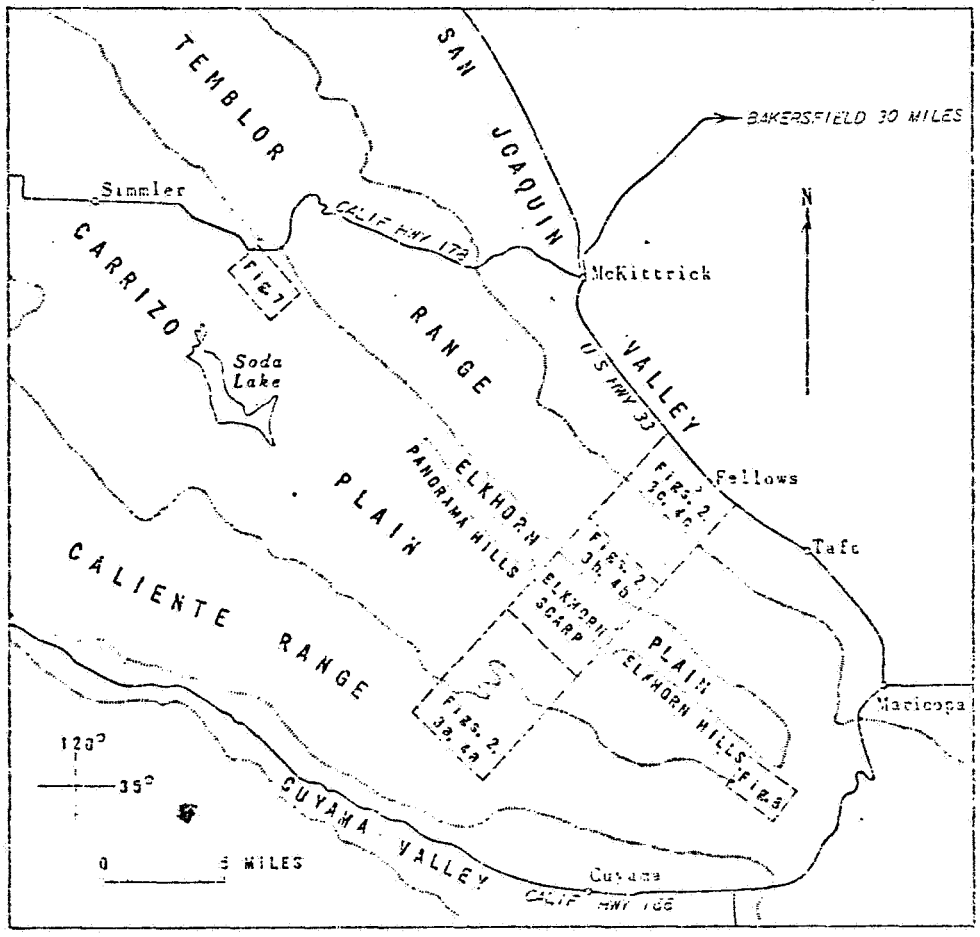

Figure 1. Index map showing major physiographic features and approximate locations of areas described and illustrated in this report.

In the image area the Caliente and Temblor Ranges are underlain by steeply dipping clastic rocks of late Tertiary age. In addition, 3 basalt flows occur within the Caliente Range sequence. The Caliente and Temblor Ranges in the image area are largely mantled by soil or debris derived from the underlying strata, and extensive outcrops of bare bedrock are rare.

Imagery

The infrared images (figures 3 and 4) are line-scan displays of the areal distribution of radiation intensities in the 8 to 13 micron wavelength band. Areas of intense radiation are relatively light in tone; those of relatively weak radiation are dark in tone in the images. Radiation intensity varies directly with emissivity and with the fourth power of absolute surface temperature. Curvature near the image margins is a distortion inherent in the scanning technique.

Figures 3, 4, and 5 near here

Figure 3 is an image made shortly before dawn (0506-0510 PDT) so that the effects of differential solar heating related to slope orientation are minimized. Figure 4 is an image made shortly after sunrise (0635-0638). In this image surfaces warmed by the sun appear relatively bright much as they would in early morning photographs. Figure 5, an aerial photograph of the northeastern part of the imaged strip, was taken from about 35,000 feet on a midsummer day.

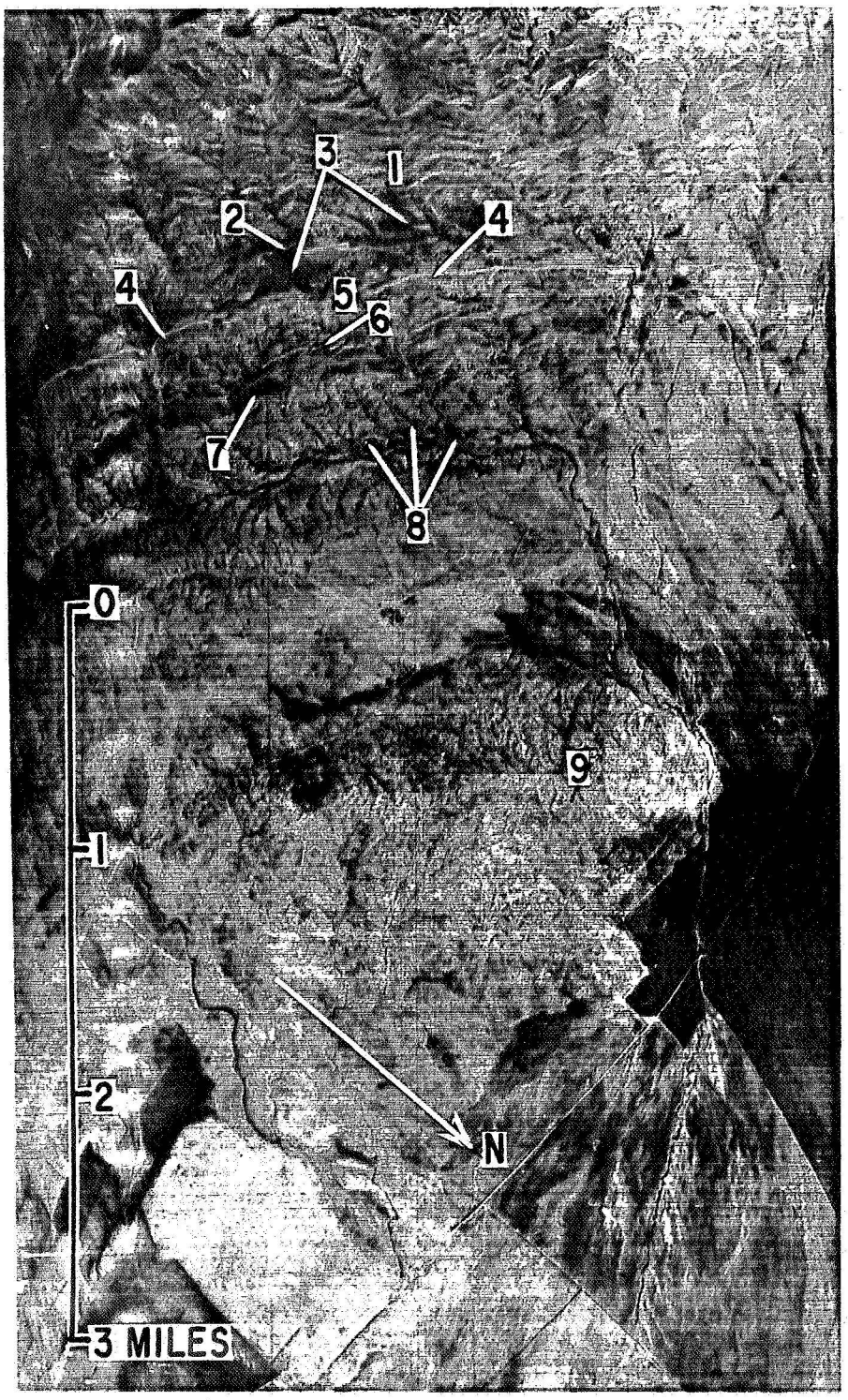

Figure 3a. Pre-dawn infrared image - Caliente Range and Carrizo Plain. See Figure 1 for location.

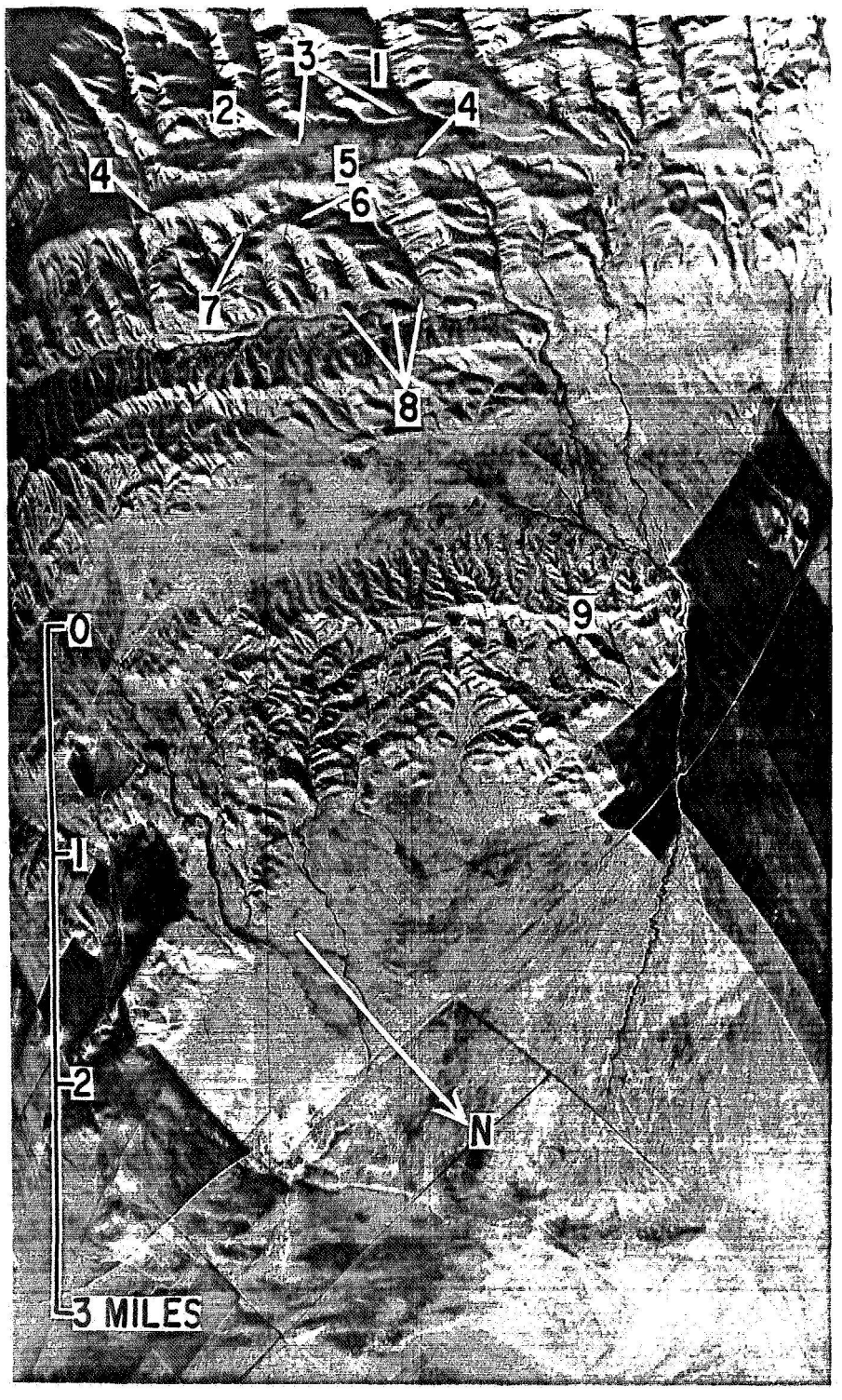

Figure 4a. Post-sunrise infrared image - Caliente Range and Carrizo Plain. See Figure 1 for location.

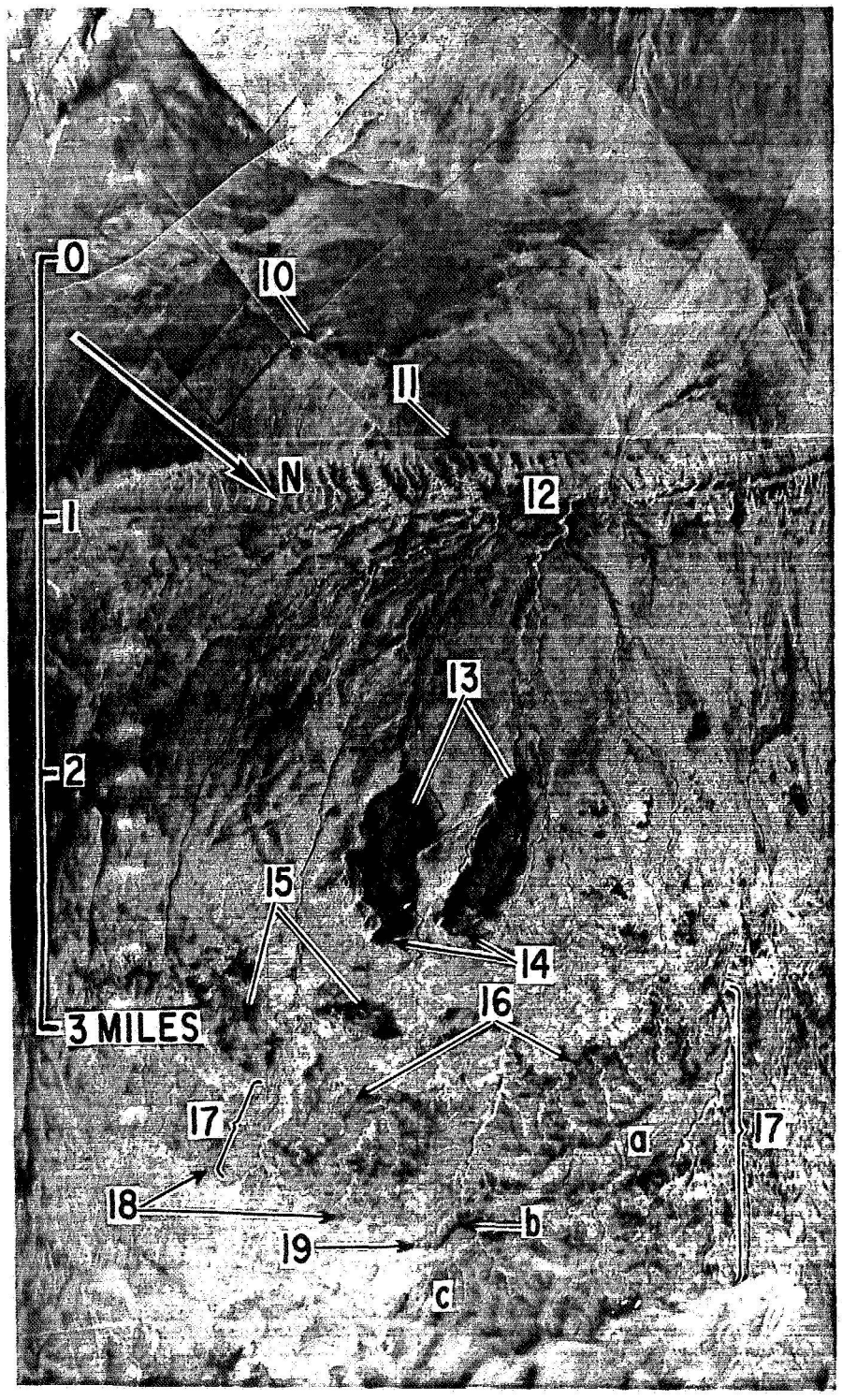

Figure 3b. Pre-dawn infrared image - Carrizo Plain, Elkhorn Plain, and Temblor Range. See Figure 1 for location.

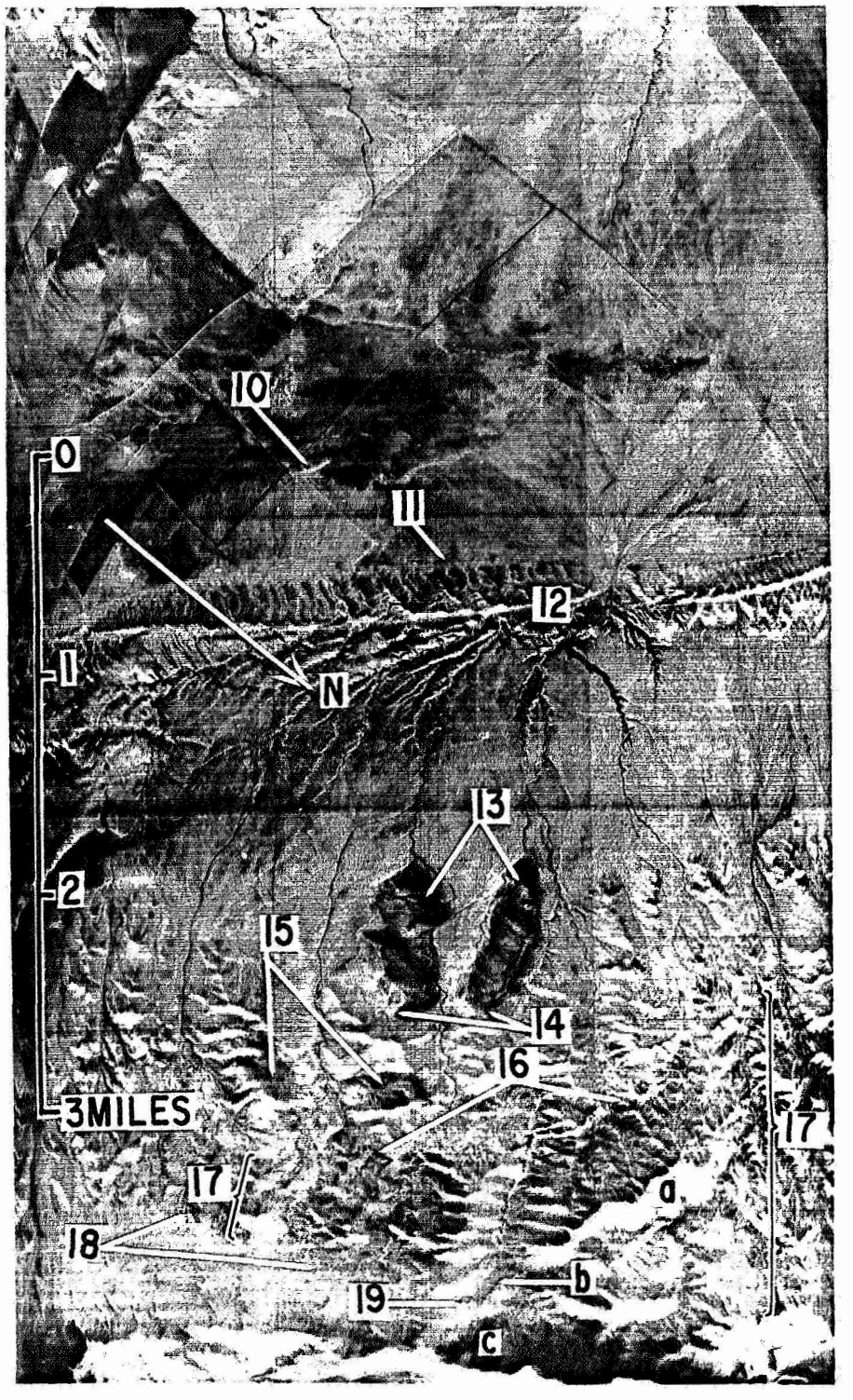

Figure 4b. Post-sunrise infrared image - Carrizo Plain, Elkhorn Plain, and Temblor Range. See Figure 1 for location.

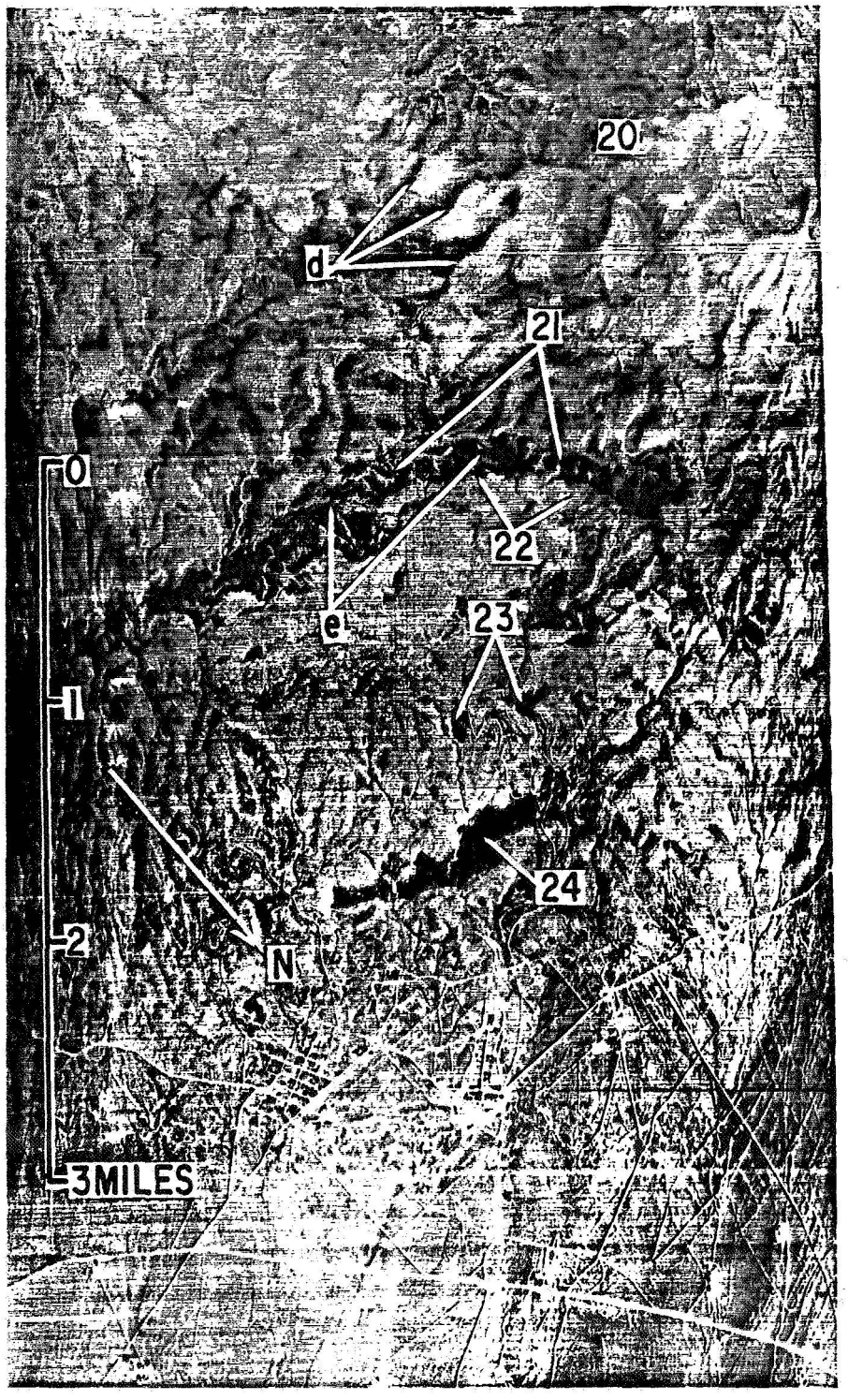

Figure 3c. Pre-dawn infrared image - Temblor Range. See Figure 1 for location.

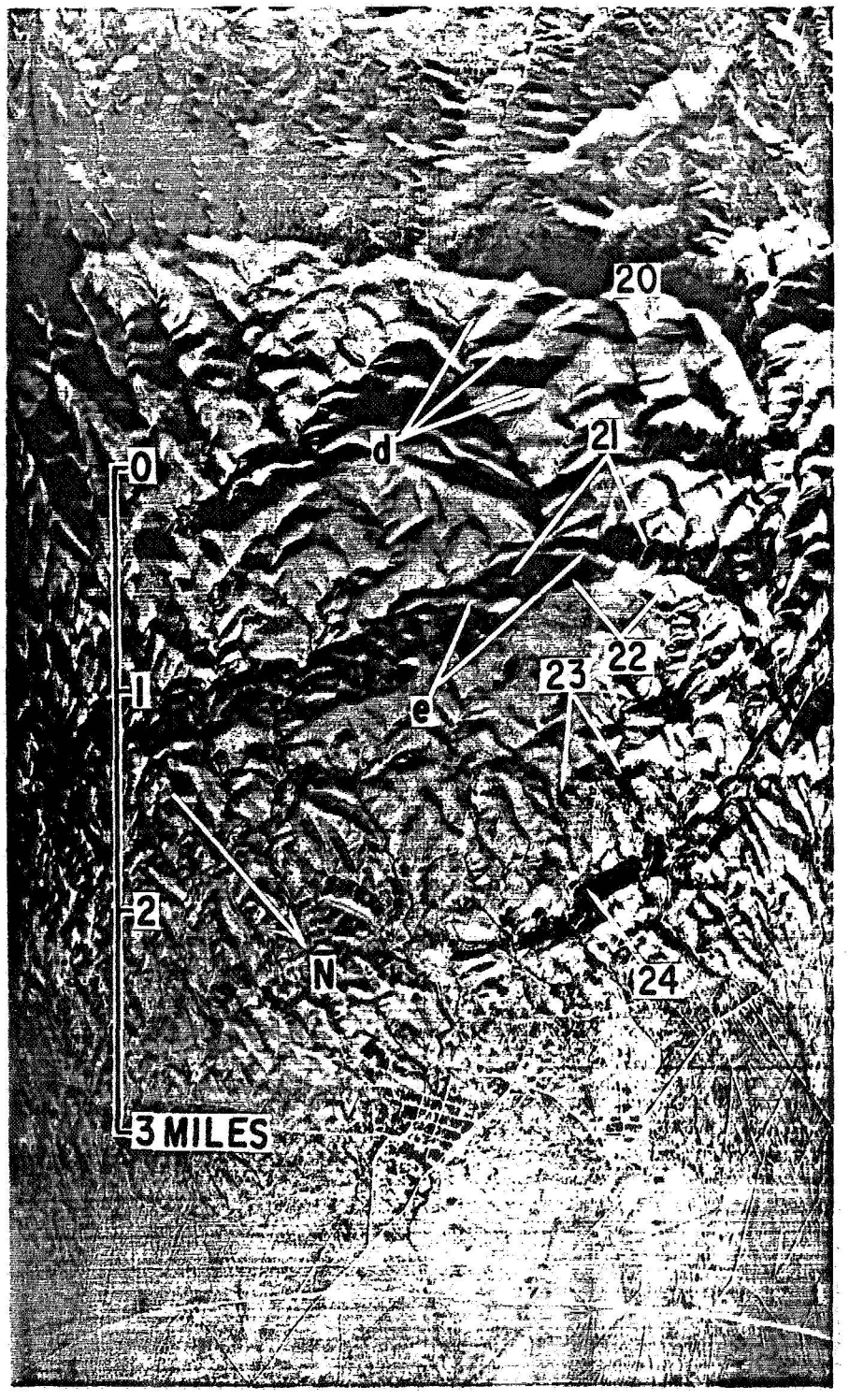

Figure 4c. Post-sunrise infrared image - Temblor Range. See Figure 1 for location.

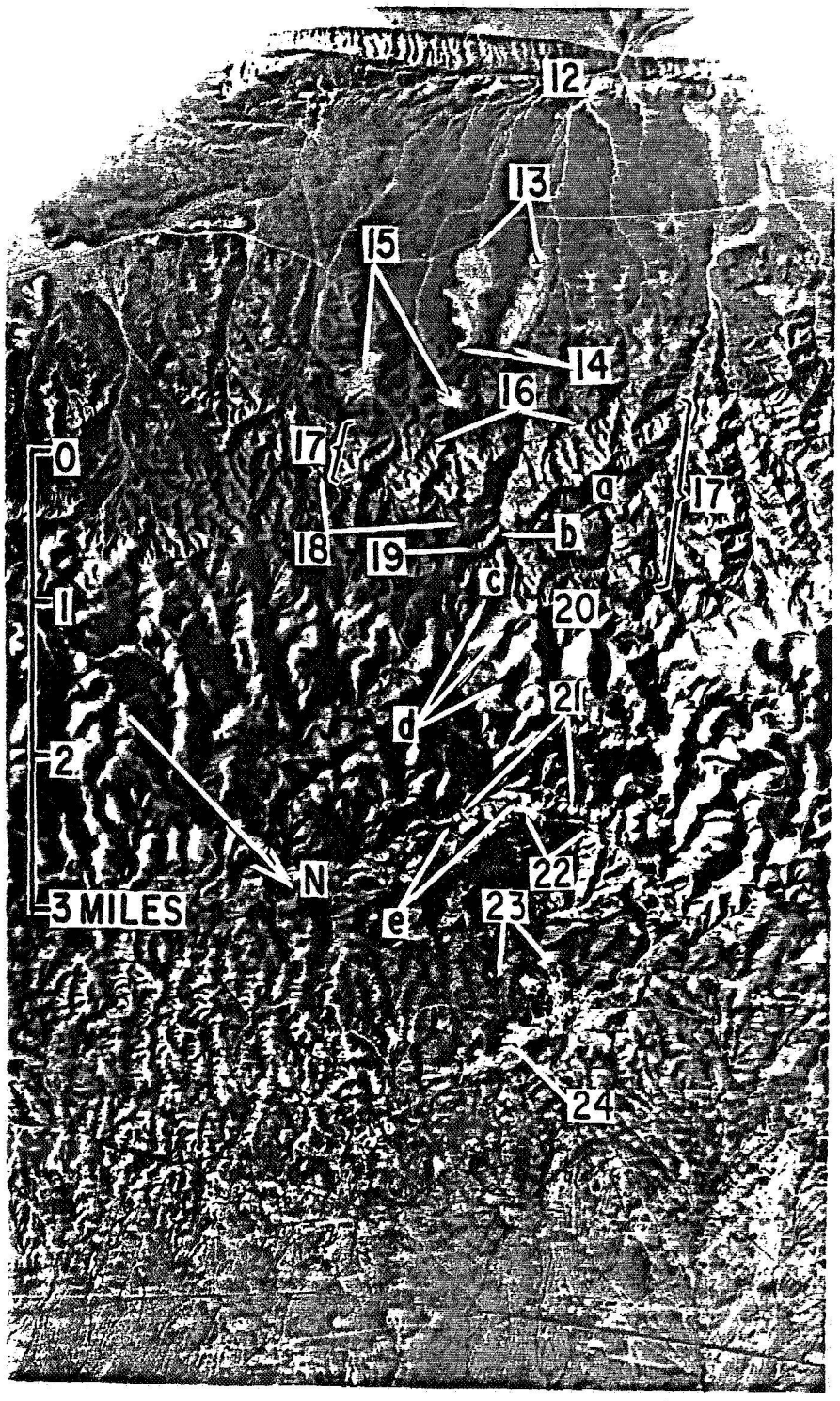

Figure 5. Small scale aerial photograph of Temblor Range southwest of Fellows.

In order to facilitate comparison and discussion, observation points are numbered on the pre-dawn and post-sunrise images (figures 3 and 4) as well as on the aerial photograph (figure 5). The annotations tabulated below are numbered to correspond to the numbers on figures 3, 4, and 5. Unless specifically noted otherwise, the annotations refer to the pre-dawn image (figure 3).

(1) Subparallel white lines coincide at least in part with local strike ridges on which bare sandstone beds and basalt flows are exposed. Pebbly texture is chapparal.

(2) White line coincides with sharp break in slope at the outer edge of a terrace mantled by old alluvium.

(3) Flat to slightly concave remnants of an old alluviated surface appear dark as do portions of nearby stream canyons.

(4) White line coincides with strike ridge on which the uppermost of three basalt flows forms a bold outcrop of bare rock.

(5) Same strike ridge as 2, but here, where the white line is indistinct, the basalt is mantled by soil and rubble.

(6) White line corresponds to bare outcrop of hard, light-colored mudstone to sandy mudstone. Adjacent bedrock mantled by soil.

(7) Dark band corresponds to the outcrop of the Quatal Formation, a mudstone consisting largely of expanding clay in contact with sandstones of the Caliente and Morales Formations.

(8) Small dark patches correspond to outcrops of reddish-brown expanding clay in Morales Formation. The bordering materials giving brighter tones are sandy soils developed on the Morales Formation and deposits of sandy and gravelly alluvium that veneer all but the small areas represented by the dark spots.

(9) Low hill underlain by claystone, sandstone, and conglomerate of the Morales Formation; bounded by broad alluviated areas. In post-sunrise imagery the hill is more distinctly outlined because of preferential heating of slopes exposed to the sun.

(10) Small hill, a few feet high, relatively bright, lies within a dark region that corresponds approximately with the lowest part of the Carrizo Plain in the image area. Images show agricultural field patterns and fan patterns where intermittent streams debouch onto the broad alluviated Carrizo Plain. Because the Carrizo Plain is nearly flat, there is almost no preferential solar heating, and the post-sunrise image closely resembles the pre-dawn image.

(11) Dark spots represent accumulations of tumbleweed against a fence at the northeast edge of the Carrizo Plain.

(12) Northwest-trending trench along recently active trace of San Andreas fault. Well drained gully bottoms, including the trench along the fault and the fine gullies forming a filigree pattern on low ridge southwest of the fault, appear bright.

(13) Two elongate hills underlain by Bitterwater Creek Shale project through the alluvial apron that underlies the Elkhorn Plain at the foot of the Temblor Range. Bitterwater Creek Shale dark in imagery but bright in aerial photograph.

(14) Bitterwater Creek Shale in contact to northeast with very coarse conglomerate of the Santa Margarita Formation. Conglomerate and alluvial apron that bounds it on the southwest are bright and contrast sharply with darkly imaged Bitterwater Creek Shale. Note that in aerial photograph the contact between Santa Margarita conglomerate and alluvium is readily apparent.

(15) Outcrops of downfolded Bitterwater Creek Shale dark; bright in aerial photograph. Geologic map (figure 2) portrays distribution of sandstone and shale mapped together as Bitterwater Creek Shale. Imagery and aerial photograph, on the other hand, display shale facies in sharp contrast to surrounding rocks whether they be Santa Margarita Formation, a sandstone facies of the Bitterwater Creek, or the alluvium of the Elkhorn Plain.

(16) Sharp radiation contact coincides with a fault separating Monterey Shale to the northeast from Santa Margarita conglomerate and a sandstone mapped with the Bitterwater Creek Shale. The conglomerate and the Bitterwater Creek sandstone, inseparable in the imagery as well as in the aerial photograph, contrast sharply with the Monterey Shale, which is dark in the pre-dawn image and light in the aerial photograph.

(17) Broad dark band occurs in an area underlain by Monterey Shale, shale and sandstone of the Temblor or Vaqueros Formation, and a sandstone unit at the base of the Santa Margarita Formation. Within the band, shale is the predominant lithology.

(18) Contact between Monterey Shale (dark in image, light in aerial photograph) and overlying Santa Margarita Formation (light in image, dark in aerial photograph).

(19) Radiation boundary at northwestern limit of conglomerate facies (light in image) of the Santa Margarita Formation within the image area. Farther northwest within the image area the Santa Margarita Formation consists predominantly of friable sandstone (dark in image) with rare granitic or metamorphic boulders. Conglomerate facies darker in aerial photograph than sandstone facies.

(20) Sharp radiation boundary coincides with crest of Temblor Range. Immediately northeast of the range crest Santa Margarita conglomerate, Media Shale, and the Temblor or Vaqueros Formations all appear bright. Most of the slope for about a mile and a half northeast of the range crest in the image area is underlain by grass-covered Monterey Shale colluvium that appears relatively bright.

(21) Dark band coincides with prominent, steep, southwest-facing slope nearly devoid of vegetation. It is underlain in part by diatomite mapped by Dibblee as Reef Ridge Formation (figure 2) and in part by Monterey Shale.

(22) Sharp radiation contact between Reef Ridge diatomite (dark in image, bright in aerial photograph) and overlying Santa Margarita conglomerate (bright in image, dark in aerial photograph).

(23) Small dark spots coincide with windows in gravel colluvium, through which Reef Ridge diatomite is exposed in the Fellows oil field.

(24) Dark band coincides with steep, barren, southwest-facing slope on which Reef Ridge diatomite is exposed. Santa Margarita conglomerate southwest of the diatomite and gravels of the Tulare Formation northeast of the diatomite appear bright. Near the northeast end of the image the community of Fellows stands on undeformed younger alluvial deposits.

Intensity of pre-dawn infrared radiation in the Temblor Range is apparently related in part to slope orientation. North-facing slopes tend to be relatively bright; south-facing slopes tend to be dark in the pre-dawn imagery (figure 3). The largest topographic feature showing this tendency is the crest of the Temblor Range. Near locality 20 a well defined radiative boundary separates similar lithologic types at the range crest. The northeast flank of the range is relatively bright, the southwest flank relatively dark. A few other examples of this tendency, denoted by letters in figures 3, 4, and 5, are listed below:

a. steep north-northeast-facing hill in Monterey Shale bright in pre-dawn imagery (figure 3); strikingly warmed by early morning sun (figure 4).

b. hill underlain by basal sandstone of Santa Margarita Formation dark on south side, bright on north side in figure 3.

c. gullied area just southwest of range crest, southeast-facing slopes dark.

d. three small ridge crests on northeast flank of range; all dark on south side and bright on north side in pre-dawn image.

e. steep northeast-facing canyon walls within dark band at locality 21 brighter than nearby southwest-facing slopes; all underlain by diatomaceous Monterey Shale.

Ground measurements

In an attempt to find systematic relationships between ground conditions and tonal densities in the pre-dawn infrared image, radiation temperature, specific gravity, and moisture data were collected late in May 1967. According to Weather Bureau records, no rain fell in the area in May or June prior to IR flight on June 18, 1965. Rainfall in April 1965 was approximately 2 inches both east of the area at Maricopa and west of the area at Cuyama. In April 1967, 1.85 inches of rain fell at Maricopa and 2.82 inches fell at Cuyama. During May 1967, 0.02 inches fell at both Cuyama and Maricopa approximately two weeks before the ground data were collected. In spite of the slightly wetter weather in the spring of 1967, the ground in late May in the area of figures 3, 4, and 5 seemed thoroughly dry and grass cover was brown.

Radiation temperatures were measured with a hand-held Barnes IT-3 radiometer over a period of two days and three nights from May 22 to 25 at two different sites near contacts between Bitterwater Creek Shale and alluvium (locality 13). Infrared radiation, the quantity measured by the radiometer, varies as emissivity and as the fourth power of the absolute temperature.

$$W = \varepsilon\sigma T^4$$

W = total radiation per unit area (8-13 micron radiation in this case)

ε = emissivity

T = absolute temperature (^{o}K)

σ = a constant

Emissivity of an object is the ratio of its emittance (radiant energy emitted per unit area) to the emittance of a perfect radiator (blackbody) at the same temperature. Blackbodies exist in theory only; real substances have emissivities smaller than 1. The radiometer measures emittance, but indicates a temperature scale based on an emissivity of 1. Because natural materials have emissivities smaller than 1, radiation temperatures are lower than true temperatures. In the temperature range in which this study was made, a change of .05 in emissivity for high emissivities produces a change of about $4^{o}C$ in apparent temperature. Greater distortion occurs with low emissivities.

Laboratory radiometer measurements of large samples of surficial material collected from Bitterwater Creek Shale, Santa Margarita conglomerate (cobbles and boulders excluded), Monterey Shale, Reef Ridge diatomite, Quatal Formation, Morales Formation, and alluvium of the Elkhorn Plain suggest that differences in radiant emittance are not caused by emissivity differences related to the compositions of the soils. Radiation temperatures of the samples, which stood for several weeks in a normally heated room, were all within 1°C of each other, with a systematic variation that was apparently related to position in the room rather than to lithology. The apparent temperatures (near 72°F) approximate room temperature and suggest that all of the samples had high emissivities.

Figure 6 displays radiation temperature data collected on typical grass-covered sandy alluvium and on barren soil developed on Bitterwater Creek Shale. The same relationship, with Bitterwater Creek Shale appearing colder both day and night, was later repeated at a second site. Radiation from alluvium with relatively sparse grass cover and from Bitterwater Creek Shale with sparse grass cover was intermediate between the extremes of barren Bitterwater Creek Shale and typically grassy alluvium both day and night. Single boulders in the alluvium were slightly more radiant in the pre-dawn hours than the deposits that included them. The radiometer measurements show that the radiation patterns recorded in the imagery are reproducible and suggest that physical properties, such as specific gravity and moisture content, that may have affected radiance when the images were made, were also effective in May 1967, when field observations were made.

Figure 6 near here

Densities and moisture contents of representative surficial materials were determined. Approximately 1,000 cc of soil from the uppermost two inches were carefully collected and immediately weighed. Volume was determined by filling the excavation with a measured quantity of sand, and density was computed. Moisture content was determined by comparing the sample weight after several days of drying at 110°C with its weight at the time of collection. Surficial materials developed on sandy alluvium, sandstone units, and on Santa Margarita conglomerate (cobbles and boulders excluded from measurements) range in density from about 1.3 to 1.5 and in moisture content from 1.6 to 2.8 per cent. Surface materials representing shale units range in density from about 1.0 to 1.1, and their moisture contents range from 5.3 to 8.4 per cent. The specific gravity of diatomite surficial debris from the east side of the Temblor Range (locality 18) is about 0.9. X-ray data show that much of the shale and mudstone is montmorillonitic; the high moisture contents may represent water driven from the clay mineral structure by heating rather than high accumulations of pore water. In late May, soils in the area of figures 3, 4, and 5 looked and felt thoroughly dry.

Synthesis

Comparison of the pre-dawn image, the aerial photograph, and the ground data suggest that intensity of pre-dawn radiance may be related to specific gravity of soil, vegetative cover, reflectivity, slope orientation, and microclimatic effects as summarized below.

Low pre-dawn radiance	High pre-dawn radiance
low specific gravity (approx. 1.0)	high specific gravity (approx. 1.3)
little or no grass cover	relatively thick grass cover
bright in aerial photograph (high reflectivity)	dark in aerial photograph (low reflectivity)
slope faces south	slope faces north
entrapment of cold air	

Soils developed on shale, mudstone, and diatomite have low specific gravities (about 1.0) and ordinarily are dark in the pre-dawn image (localities 7, 8, 13, 14, 15, 16, 17, 18, 21, 23, 24). The same soils generally support little or no grass cover and reflect sunlight relatively intensely as shown by the aerial photograph. In contrast, soils developed on Santa Margarita conglomerate, most sandstone units, and sandy alluvium have higher specific gravities (about 1.3) and tend to be bright in the pre-dawn image (localities 8, 14, 15, 16, 18, 22). They support more vegetation than the shales and reflect less sunlight as shown by their darkness in the aerial photograph. In addition, south-facing slopes tend to be less radiant in the pre-dawn image than north-facing slopes. Hence, the intensity of pre-dawn radiance from any surface may be controlled by several factors. Microclimatic effects related to nocturnal density stratification of air apparently produce additional local radiative anomalies that are discussed later.

Specific gravity.--Specific gravity of surficial material plays an important role in determining its thermal inertia, which is a measure of resistance of its surface to temperature change.

$$\text{Thermal inertia} = K\rho C$$

K = thermal conductivity

ρ = specific gravity

C = specific heat

Surface materials with high thermal inertia react slowly to external temperature changes and, other factors being equal, should be warmer in the pre-dawn hours than surficial materials with low thermal inertia.

Materials with high thermal conductivity transmit heat relatively easily and change in surface temperature relatively slowly in response to a change in external temperature. Air, water, and solid rock increase in thermal conductivity approximately in the ratio 1:25:90. Hence dry porous material has relatively low thermal conductivity and the surface temperature changes quickly in response to external temperature changes. Specific heat, a measure of heat input necessary to produce a given temperature increase, is about five times as high for water as for air or mineral grains. Insofar as an inverse relation exists between specific gravity and porosity in the surficial materials of the image area, thermal conductivity, thermal inertia and, hence, pre-dawn radiance increase with specific gravity.

In addition to the relationship previously noted between soil of low specific gravity and low pre-dawn radiance, the following observations support the correlation between specific gravity and pre-dawn radiance:

(1) Outcrops of bare bedrock (localities 1, 4, 6) with specific gravities much higher than those of the surrounding soils are displayed in the imagery as bands of high pre-dawn radiance. It should be noted that a similar band (locality 2) apparently coincides only with a sharp break in slope.

(2) As indicated by radiometer measurements in the pre-dawn hours, single boulders were slightly more radiant than the unconsolidated alluvium that surrounded them.

(3) Tumbleweed piled along a fence at locality 11 forms a surficial material that, because of its extremely low specific gravity and high porosity, has low thermal inertia and appears dark in the pre-dawn image.

(4) Wallace and Moxham (1966, 1967) showed that unplowed fields in some other Carrizo Plain images were brighter in the pre-dawn than plowed fields. Plowing, by increasing the porosity and lowering the specific gravity of soil, lowers its thermal inertia.

Grass cover and reflectivity.--Radiometer measurements (figure 6) in late May showed that Bitterwater Creek Shale at locality 13 was less radiant than the adjacent alluvium both day and night, an unlikely situation if thermal inertia were the sole controlling influence. Perhaps vegetative cover and (or) reflectivity influence radiance in one of the following ways:

(1) Figure 6 shows radiometer measurements on typically barren shale and on typically grass alluvium. Radiant temperatures on slightly grassy shale and on alluvium with relatively thin grass cover were intermediate between the extremes shown in figure 6. Gates (1964, p. 576) states that all plant surfaces have emissivities of 0.95 or greater and most leaf emissivities are 0.97 to 0.98. It may be that the grass-covered surfaces are slightly higher in emissivity than the barren surfaces. Under the existing conditions an increase in emissivity of 0.05 would produce a radiant temperature increase of about $4^{\circ}C$, a temperature difference consistent with the radiometer results.

(2) Possibly the Bitterwater Creek Shale, bright in the aerial photograph, absorbs less heat then the surrounding alluvium in the daytime because of its relatively intense reflection of solar radiation. Elsewhere in the study area, south slopes underlain by shale tend to be relatively barren and to reflect solar radiation more intensely than adjacent areas underlain by sandstone, conglomerate, and alluvium.

The barren shales, in addition to absorbing less energy from incoming solar radiation, may cool more rapidly at night because of relatively low thermal inertia. Probably thermal inertia, vegetative cover, and reflectivity interact complexly in controlling pre-dawn radiance throughout the image area.

Slope orientation.--North slopes in the Temblor Range are more radiant in the pre-dawn image than nearby south slopes underlain by similar lithologies. In some places, vegetation is more lush on north slopes than on south ones, but the relationship is not consistent. Untested hypotheses include the possibility that slightly higher moisture content in soils on north slopes may have caused slightly higher thermal inertia or that atmospheric interference such as high clouds to the north at the time of the flight could have impeded radiation to space from the north slopes.

Microclimatic effects.--In addition to the influences of specific gravity, vegetative cover, and slope orientation on image tonal densities, microclimatic effects related to local topographic features apparently influence pre-dawn ground temperature and cause radiative anomalies. Low pre-dawn radiance at localities 3 and 10 is attributed to nocturnal accumulation of cold air on poorly drained ground surfaces, a phenomenon extensively documented by Geiger (1957). The diamond-shaped dark area at locality 3 in figure 3 is a flat surface, or possibly even a shallow closed depression, partially enclosed by surrounding hills. The surface is underlain by old alluvium, which is sandy and closely resembles in both texture and vegetative cover other alluvial deposits that appear bright in figure 3. The suggested interpretation of the diamond-shaped area is that it represents an area in which cold air accumulates preferentially at night and the surface beneath the colder air becomes slightly cooler than nearby surfaces. A similar interpretation is suggested at locality 10, where the dark region in the image coincides approximately with the lowest part of the valley floor in the image area. A small hill projecting through the colder air strata is slightly warmer and appears brighter in figure 3.

Gullies at locality 12 appear bright in pre-dawn image, and surface temperatures were no doubt warmer than on the adjacent interfluves. Although they are local topographic lows, the gullies may be well drained relative to air flow so that they do not permit development of the stagnation by which a thick cold air layer accumulates.

The hypothesis that entrapment of cold air causes radiative anomalies was documented in an effort to test the suggestion that some dark anomalies in pre-dawn imagery represent high soil moisture (Wallace and Moxham, 1966; Sabins, 1967, p. 749). Two areas cited by Wallace and Moxham as places where low radiation might reflect high soil moisture content were selected for study.

Figure 7 is a pre-dawn infrared image of a site located along the

---

Figure 7 near here

San Andreas fault east of Soda Lake. The rectangular pattern is a network of subdivision roads. A recently active trace of the San Andreas fault is bounded on the southwest by a scarp, the crest of which is bright in the image. The ground surface to the northeast slopes toward the scarp, and the area represented by the dark band is the topographically lowest area northeast of the scarp. Tumbleweed which has accumulated against the scarp is imaged as a thin very dark band bounding the bright scarp on the northeast. In late May 1967, the grass was green and the soil visibly damp in places at the foot of the scarp. Moisture measurements in late October 1967 showed 3 percent soil moisture at the top of the scarp and 7 percent at the base. Radiometer readings in late October showed an apparent temperature of 8°C on the scarp crest and 5°C at the base.

Pre-dawn air temperature was measured at 1, 16, and 31 inches above the ground at the scarp crest, scarp base, and in between. The data, summarized in Table 1, show that at any point stratification of the air is strongly developed, and that the air becomes appreciably colder as one moves down the scarp. The low area is a trap for cold air, which lowers the local ground temperature. The high radiant temperature ($5^{o}C$) at the base of the scarp may indicate that the relatively tall grass there projected through the coldest air layers into the overlying warmer air.

TABLE 1 near here

Table 1

Height above ground-inches	Top of scarp °C	Middle of scarp °C	Base of scarp °C
31	9.5	7.5	5.5
16	9	7	4
1	7	6	1
Ground temp. by radiometer	8		5

Table 1.--Air and ground temperatures measured along San Andreas fault east of Soda Lake, October 25, 1967 - 4:30 a.m. Air temperatures by thermometer; ground temperatures are radiation temperatures measured by Barnes IT-3 radiometer.

Figure 8 is a pre-dawn image of a second site near the southeast end of the Carrizo Plain. The dark roughly triangular area in the center of the image is a flat, in part closed, alluvial surface bounded on the northwest and southeast by low gravel hills that are bright in the image. The semi-circular bright feature overlapping the southwest flank of the dark triangular area is an alluvial fan. The flat bottom of the depression and the surrounding hills appear extremely dry. Much of the depression floor is barren of grass, and there are no visible signs of moisture. Soil moisture measurements show 2 percent moisture at the crest of one of the gravel hills and 4 percent on the flat surface below. However, the flat surface is floored by fine grained clay-rich sediment, and the slightly higher moisture content can probably be accounted for as water driven out of clay minerals by heating. Pre-dawn temperature measurements showed well developed air stratification with air temperatures 2 to 4°C lower at ground level on the flat than at ground level on the low gravel hills. The low flat area is poorly drained relative to air flow and permits the accumulation of a layer of dense cold air.

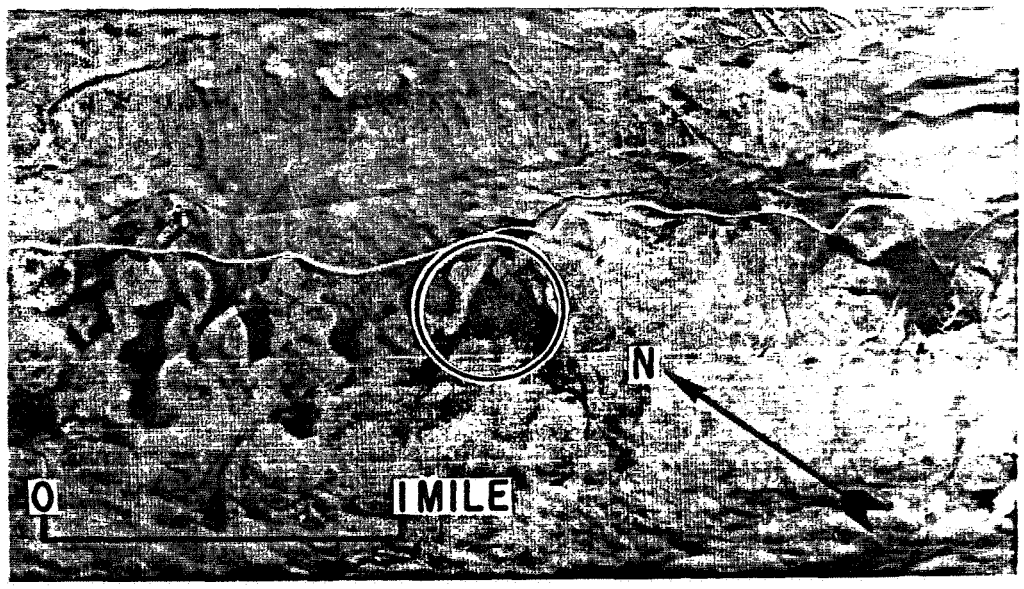

Figure 8. Pre-dawn infrared image near southeast end of Carrizo Plain. See Figure 1 for location. Observations described in text were made within circled area.

Measurements made by A. O. Waananen and C. T. Snyder (unpublished data) indicate that pre-dawn evaporation of water in arid regions is vanishingly small and cast doubt on hypotheses that radiative anomalies such as that in figure 8 reflect high soil moisture content. Evaporation from an open water surface in a 4-foot diameter evaporating pan was measured continuously for several days in late July 1963. The pan was set on a playa surface near Coaldale, Nevada. Air temperature 5 feet above the playa surface ranged from about 14°C at night to 38°C in the daytime. Relative humidity, also measured at an altitude of 5 feet was extremely low, ranging from approximately 0 in the daytime to 25 percent at night. Total daily evaporation averaged about 0.4 inch, but evaporation from the open pan between midnight and 6 a.m. totalled less than 0.05 inch.

In view of the very low pre-dawn evaporation from an open water surface in the extremely dry atmosphere of the Nevada playa, it seems doubtful that the radiative anomaly of figure 8, where surface moisture content was at most a few percent, was a product of evaporative cooling. In addition, the effect of high soil moisture on thermal inertia would act to inhibit nocturnal cooling, and, in the absence of significant evaporative cooling, moist soils might be warmer than dry soils in the pre-dawn hours. It seems most likely that the radiative anomalies of figures 7 and 8 are predominantly responses to microclimatic effects created by preferential accumulation of cold air.

Conclusions

Tonal densities in this thermal infrared imagery may reflect in part the specific gravities of surficial materials. Surficial materials with relatively high specific gravities tend to be bright in the pre-dawn image. However, effects related to atmospheric conditions, topographic setting, and vegetation may also produce marked anomalies in the imagery. Futhermore, even in the relatively well exposed geology of the Caliente and Temblor Ranges, the imagery was largely controlled by properties of soil - not bedrock. Lithologic inferences based on qualitative comparisons of radiation from soils, with the radiation complexly modified by topographic, atmospheric, and vegetative effects, are difficult.

The pre-dawn imagery shows many geologic features such as outcrop patterns and faults that are also discernible in aerial photographs. Because of the potential of infrared imagery to display microclimatic anomalies, it might be a valuable adjunct to other types of imagery in mapping geologic features such as recently active faults that have very subtle topographic expression.

It has been suggested that anomalously weak pre-dawn radiation might indicate soil moisture concentrations related to shallow ground water in low areas between landslide lobes or in areas where faults might act as barriers to groundwater (Wallace and Moxham, 1966, 1967; Sabins, 1967, p. 749). Two anomalies of this type were investigated and may have been produced largely, if not entirely, by density stratification of air.

Post-sunrise imagery shows the strong influence of solar warming of surfaces exposed to the sun. Topography is the dominant control of tonal densities in the image, which resembles a low sun angle photograph.

References

Dibblee, T. W., Jr., 1962, "Displacements on the San Andreas rift zone and related structures in Carrizo Plain and vicinity [California], in Guidebook, Geology of Carrizo Plains and San Andreas Fault," San Joaquin Geol. Soc. and Am. Assoc. Petroleum Geologists - Soc. Econ. Paleontologists and Mineralogists. Pacific Sec. [field trip], 1962, p. 5-12.

Gates, D. M., 1964, "Characteristics of soil and vegetated surfaces to reflected and emitted radiation," Symposium Remote Sensing of Environment, 3d, Michigan Univ., Ann Arbor, Infrared Physics Lab., Proc., p. 573-600.

Geiger, R. E., 1957, The climate near the ground, 2d, ed., Harvard Univ. Press, Cambridge, Mass., 494 pp.

Sabins, F. F., Jr., 1967, "Infrared imagery and geologic aspects," PHOTOGRAMMETRIC ENGINEERING, v. 33, no. 7, p. 743-750, July 1967.

Vedder, J. G., and Repenning, C. A., 1965, "Geologic map of the southeastern Caliente Range, San Luis Obispo County, California," U.S. Geol. Survey Oil and Gas Inv. Map OM-217, scale 1:24,000.

Wallace, R. E., and Moxham, R. M., 1966, "Use of infrared imagery in study of the San Andreas fault system, California," U.S. Geol. Survey Tech. Letter NASA-42; 1967, Use of infrared imagery in study of the San Andreas Fault system, California, in Geological Survey Research 1967, U.S. Geol. Survey Prof. Paper 575-D, P. D147-D156; abs. in Symposium Remote Sensing of Environment, 4th, Michigan Univ., Ann Arbor, Infrared Physics Lab., Abstracts, p. 24.